

# Automatic segmentation of epidural hematomas using a computational technique based on intelligent operators: a clinical utility

*Segmentación automática de hematomas epidurales usando una técnica computacional, basada en operadores inteligentes: utilidad clínica*

Juan Salazar MSc<sup>1</sup>, <https://orcid.org/0000-0001-6826-203X>, Miguel Vera MSc, PhD<sup>1,2\*</sup>, <https://orcid.org/0000-0001-7167-6356>, Yoleidy Huérfano MSc<sup>2</sup>, <https://orcid.org/0000-0003-0415-6654>, Oscar Valbuena MSc<sup>3</sup>, <https://orcid.org/0000-0003-3080-8839>, Williams Salazar MD<sup>4</sup>, <https://orcid.org/0000-0001-5669-6105>, María Isabel Vera BSc<sup>4</sup>, <https://orcid.org/0000-0003-1135-6283>, Elkin Gelvez MSc<sup>1</sup>, <https://orcid.org/0000-0001-5157-3341>, Yudith Contreras MSc<sup>1</sup>, <https://orcid.org/0000-0003-4358-730X>, Maryury Borrero MSc<sup>1</sup>, <https://orcid.org/0000-0003-3025-1321>, Marisela Vivas MSc, PhD<sup>5</sup>, <https://orcid.org/0000-0002-8941-4562>, Doris Barrera MSc<sup>1</sup>, <https://orcid.org/0000-0002-6443-6757>, Carlos Hernández MSc<sup>1</sup>, <https://orcid.org/0000-0001-8906-1982>, Ángel Valentín Molina MSc<sup>6</sup>, <https://orcid.org/0000-0001-9604-7222>, Luis Javier Martínez PhD<sup>7</sup>, <https://orcid.org/0000-0003-0917-9847>, Frank Sáenz MSc<sup>7</sup>, <https://orcid.org/0000-0001-9604-7220>

<sup>1</sup>Universidad Simón Bolívar, Facultad de Ciencias Básicas y Biomédicas, Cúcuta, Colombia.

\*E-mail de correspondencia: [m.avera@unisimonbolivar.edu.co](mailto:m.avera@unisimonbolivar.edu.co)

<sup>2</sup>Grupo de Investigación en Procesamiento Computacional de Datos (GIPCD-ULA), Universidad de Los Andes-Táchira, Venezuela.

<sup>3</sup>Grupo de Investigación en Educación Matemática, Matemática y Estadística (EDUMATEST), Facultad de Ciencias Básicas, Universidad de Pamplona.

<sup>4</sup>Servicio de Neurología, Hospital Central de San Cristóbal- Táchira, Venezuela.

<sup>5</sup>Universidad Simón Bolívar, Departamento de Ciencias Sociales y Humanas, Cúcuta, Colombia.

<sup>6</sup>Grupo de Investigación en Ingeniería Clínica - HUS (GINIC-HUS), Vicerrectoría de Investigación, Universidad ECCI.

<sup>7</sup>Universidad Simón Bolívar, Facultad de Ingeniería, Cúcuta, Colombia

## Abstract

This paper proposes a non-linear computational technique for the segmentation of epidural hematomas (EDH), present in 7 multilayer computed tomography brain imaging databases. This technique consists of 3 stages developed in the three-dimensional domain, namely: pre-processing, segmentation and quantification of the volume occupied by each of the segmented EDHs. To make value judgments about the performance of the proposed technique, the EDH dilated segmentations, obtained automatically, and the EDH segmentations, generated manually by a neurosurgeon, are compared using the Dice coefficient (Dc). The combination of parameters linked to the highest Dc value, defines the optimal parameters of each of the computational algorithms that make up the proposed nonlinear technique. The obtained results allow the reporting of a Dc superior to 0.90 which indicates a good correlation between the manual segmentations and those produced by the computational technique developed.

Finally, as an immediate clinical application, considering the automatic segmentations, the volume of each hematoma is calculated considering both the voxel size of each database and the number of voxels that make up the segmented hematomas.

**Keywords:** Brain Tomography, Epidural Hematomas, Nonlinear Computational Technique, Smart Operators, Segmentation.

## Resumen

Este artículo propone una técnica computacional no lineal para la segmentación de los hematomas epidurales (EDH), presente en 7 bases de datos de imágenes cerebrales de tomografía multicapa. Esta técnica consta de 3 etapas desarrolladas en el dominio tridimensional, a saber: preprocesamiento, segmentación y cuantificación del volumen ocupado por cada uno de los EDH segmentados. Para hacer juicios de valor sobre el rendimiento de la técnica propuesta, las segmentaciones dilatadas de EDH, obtenidas automáticamente, y las segmentaciones de EDH, generadas manualmente por un neurocirujano, se comparan utilizando el coeficiente de Dice (Dc). La combinación de parámetros vinculados al valor más alto de Dc define los parámetros óptimos de cada uno de los algoritmos computacionales que conforman la técnica no lineal propuesta. Los resultados obtenidos permiten el reporte de un Dc superior a 0.90 que indica una buena correlación entre las segmentaciones manuales y las producidas por la técnica computacional desarrollada. Finalmente, como aplicación clínica inmediata, considerando las segmentaciones automáticas, el volumen de cada hematoma se calcula considerando tanto el tamaño del vóxel de cada base de datos como el número de vóxeles que conforman los hematomas segmentados.

**Palabras clave:** Tomografía cerebral, Hematomas epidurales, Técnica computacional no lineal, Operadores inteligentes, Segmentación.

## Introduction

The segmentation of anatomical structures of the human brain, present in images acquired by any imaging modality, constitutes the starting point for the diagnosis of a large number of diseases or pathologies that affect the brain; among these are intracranial hematomas which can be classified in various ways<sup>1,2</sup>. It is a known fact that digital neural images are accompanied by varied imperfections such as noise and artifacts<sup>3,4,5</sup>. These imperfections become real challenges, when computational strategies are implemented to generate the morphology (normal or abnormal) of the mentioned structures.

Reviewing the state of the art regarding segmentation of EDH's, the works described below were found. Liao et al.<sup>6</sup> describe an automatic computational technique for the segmentation of cerebral hematomas, considering the modality of multiscale computer tomography (MSCT). This technique consists of: a) Application of a filtering stage, based on the maximum filter (MaxF) and the mean filter (MF). b) Use of multiresolution Gaussian pyramids (MRGP) generated from the filtered images. c) Implementation of multiresolution level sets (MRLS) to obtain the EDH segmentations. They report an average Dice coefficient<sup>7</sup> of 0.9140 for the segmented EDHs.

Recently, Kamnitsas et al.<sup>8</sup>, reported an automatic technique based on convolutional neural networks, that apply deep learning, for the segmentation of space-occupying lesions that include EDHs present in multimodality medical images. They report a Dice Coefficient (Dc) greater than 0.90 in the segmentation of this type of injury.

In the work presented in this paper we describe a non-linear computational technique (NLCT) for the segmentation of epidural hematomas, as shown in 7 databases conformed by three-dimensional brain images of MSCT. This technique involves the stages of pre-processing, segmentation, post-processing and quantification of EDH, via volume occupied by the hematoma in the skull.

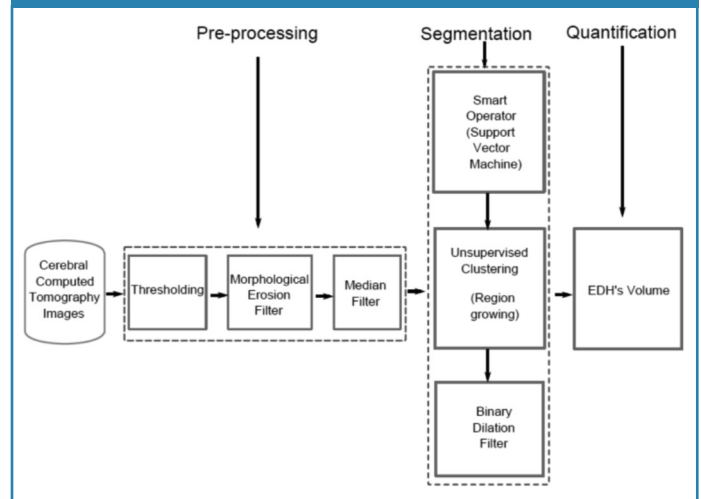
## Materials and methods

**A. Database:** The databases (DB) used were supplied by the Central Hospital of San Cristóbal-Táchira-Venezuela. They were acquired through the MSCT modality and are constituted by three-dimensional images (3D), corresponding to the anatomical structures present in the head of 7 male patients.

### B. Proposed computational technique for the automatic segmentation of epidural hematomas

In figure 1, a schematic diagram synthesizes the methods that make up our proposed technique, to segment the aforementioned hematomas.

Figure 1. Block diagram of the NLCT proposed for epidural hematomas segmentation.



### C. Pre-processing stage:

**Defining a volume of interest (VOI) which contains each hematoma to be considered:** In figure 1, the phase which establishes a volume of interest corresponds to the block called Thresholding. Thresholding algorithms are, generally, simple structures and allow for efficient classification of the elements of an image considering one or more thresholds<sup>9</sup>. In the present work simple thresholding was used, allowing for discrimination between the anatomical structure of interest and the rest of the structures present in an image<sup>9,10</sup>.

**Filtering phase:** In the block diagram, presented in figure 1, this phase corresponds to the morphological erosion and median filters. A brief explanation of both filters follows.

#### - Morphological Erosion Filter (MEF):

In practice, Mathematical morphology<sup>11,12</sup> is implemented through various morphological filters whose basic operators are erosion and dilation<sup>13</sup>. These operators are non-linear spatial filters that can be applied to binary, gray-scale or color images. In particular, the erosion ( $\ominus$ ) of a two-dimensional image ( $I$ ), composed of gray levels, using a two-dimensional structuring element ( $SE$ ), as shown in Equation 1<sup>14,15</sup>.

$$(I \ominus SE)(x, y) = \min_{(s,t) \in B} [I(x + s, y + t) - SE(s, t)] \quad (1)$$

Where  $\min$  is the minimum gray level contained in  $SE$ ,  $(s, t)$  and defines the size of the  $SE$  and  $(x, y)$  represents the position of the pixel under study.

#### - Median Filter (MF):

The median filter (MF) is also non-linear and it is used normally to minimize the impulsive-type noise present in the gray levels of the voxels neighboring the voxel object of study<sup>16</sup>. This type of filter is characterized by the conservation of the edges of the objects present in the image and it has the advantage that the final value, of the voxel, is a real value present in the image and not an average. In addition,

the median filter is less sensitive to extreme values. One of the main drawbacks is that the computation time increases, substantially, as the size of the neighborhood increases<sup>17</sup>.

#### D. Segmentation stage

##### - Computer intelligence operators: Support vector machines (SVM).

Support vector machines (SVM) are paradigms that undergo training and detection processes, and are based on both the Vapnik-Chervonenkis learning theory and the minimization principle that considers structural risk<sup>18</sup>. SVMs can be considered as classification and functional approach tools<sup>19,20</sup>.

A variant of the SVM, called the least squares support vector machine (LSSVM), can be obtained using robust statistics, Fisher discriminant analysis and replacing the inequation system that governs the SVM, by an equivalent system of linear equations, which can be solved more efficiently<sup>21,22,23</sup>.

In this work, the location of the seed voxel, to initialize the segmentation technique called Region Growing<sup>16</sup> (RG), is calculated using LSSVM. For the purposes of this work, a radial base function (RBF) is considered in the LSSVM as the decision surface and, therefore, a formulation is obtained that depends on the hyperparameters identified as: a) Error penalty parameter ( $\gamma$ ) and b) a parameter to control the selectivity ( $\sigma^2$ ) of the LSSVM.

In order to identify automatically the coordinates of the seed voxel, the following procedure was implemented:

- i) A size reduction technique is applied, based on bicubic interpolation, optimal reduction factor, is matched with that obtained in [3]. The results of this reduction are sub-sampled images of 64x64 pixels from filtered images of 512x512.
- ii) A neurosurgeon selects, on the sub-sampled image, a reference point (P1) given by the centroid of the layer containing the maximum blood pool occupied by the EDH. For this point, the manual coordinates that unambiguously establish their spatial location in each considered image are identified.
- iii) A LSSVM is implemented to recognize and detect point P1. For this, the processes of:

**Training.** Training circle circular neighborhoods of 10 pixels are selected, manually traced by a neurosurgeon, containing both point P1 (markers) and regions not containing P1 (no markers) are selected as a training set.

Then, each neighborhood is vectorized and, considering its gray levels, the attributes are calculated: mean, variance, standard deviation and median. Thus, both markers and non-markers are described by vectors ( $\mathbf{V}_a$ ) of statistical attributes, given by:  $\mathbf{V}_a = [\text{mean, variance, standard deviation and median}]$ . Additionally, the LSSVM is trained considering the vectors  $\mathbf{V}_a$  as a training pattern and intoning the values of the parameters that control its performance,  $\gamma$  and  $\sigma^2$ .

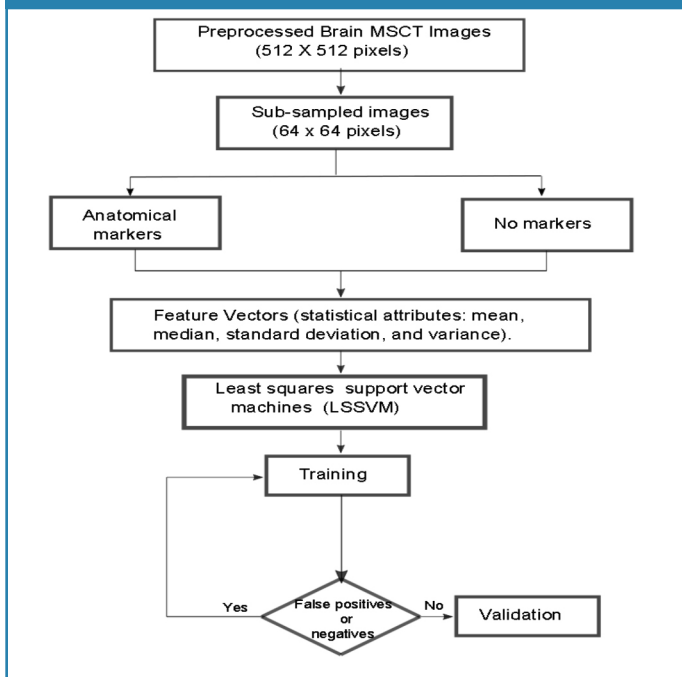
The training set is constructed with a ratio of 1:10, which means that 10 non-markers are included for each marker. During training, a classifier with a decision boundary is generated to detect LSSVM entry patterns as markers or non-markers. Subsequently, due to the presence of false positives and negatives, a process is applied that allows incorporating into the training set the patterns that the LSSVM initially classifies inappropriately.

In this sense, we considered a toolbox called LS-SVMLAB and the Matlab15 application to implement an LSSVM classifier based on a radial base gaussian kernel with parameters  $\sigma^2$  and  $\gamma$ .

**Validation.** The trained LSSVMs are used to detect P1, in images not used during training. To do this, a trained LSSVM looks for this reference point, in the axial view, from the first to the last image that makes up each of the 7 databases considered.

Finally, as a synthesis, figure 2 illustrates the process followed to locate the seed voxel in the databases considered.

Figure 2. Synthetic diagram that illustrates the operation of the LSSVM for the detection of seed voxel coordinates.



##### - Unsupervised clustering: Region Growing (RG).

Region Growing is an unsupervised grouping technique, which performs an iterative process that tries to characterize each of the classes, according to the similarity between the voxels that integrate every one of them and thus perform the segmentation<sup>16</sup>. The RG requires a “seed” point which can be selected, manually or automatically, to extract all the pixels connected to it<sup>16</sup>. To apply the RG, to the pre-processed images, the following considerations were made: a) The initial neighborhood, which is constructed from the seed, is assigned a cubic shape whose side depends on an arbitrary scalar  $r$ . The  $r$  parameter requires an intonation process. b) As a pre-defined criterion, modeling is chosen through Equation 2.

$$\|x\| - \mu < m\sigma \quad (2)$$

Where  $I(x)$  is the intensity of the seed voxel,  $\mu$  and  $\sigma$  the arithmetic mean and the standard deviation of the gray levels of the initial neighborhood and  $m$  a parameter that requires intonation.

- **Binary dilation filter**

In order to compensate the effect produced by the morphological erosion filter, the application of a morphological dilation filter (MDF) is considered, taking into account the binary image obtained by RG. The effect of morphological dilation is to enlarge the regions of the maximum intensity image. In particular, the dilation ( $\Theta$ ) of a two-dimensional binary image ( $I_b$ ), using a bidimensional structuring element ( $B$ ), is defined as the result of operating the  $I_b$  with the values of the SE under the logical operation OR<sup>14</sup>. For the purposes of this work, a cubic structuring element was considered and the size of said SE left as a parameter to control the performance of the dilatation process.

- **Tuning parameters: Obtaining optimal parameters**

The adequate performance of the proposed technique requires obtaining optimal parameters for each of the algorithms that comprise it. To do this, Database 1 (DB1) was used as a reference, the parameters to be tuned associated with the technique are modified by systematically going through the values belonging to certain ranges, as described below.

The erosion, median and expansion filters have as parameter the size of the observation window. In order to reduce the number of possible combinations, an isotropic approach was considered so as to establish the range of values which control the size of the window, which is given by the odd combinations, given by the following ordered lists: (1,1,1), (3,3,3), (5,5,5), (7,7,7) and (9,9,9).

The parameters of the LSSVM,  $\sigma^2$  and  $\gamma$ , are toned assuming that the cost function is convex and developing tests based on the following steps:

In order to tone the parameter  $\gamma$ , the value of  $\sigma^2$  is arbitrarily set and values are systematically assigned to the parameter  $\gamma$ . The value of  $\sigma^2$  is initially set at 2.5. Now,  $\gamma$  is varied within the range [0,100] with a step size of 0.25. An analogous process is applied to tone the parameter  $\sigma^2$ ; that is,  $\gamma$  is assigned the optimal value obtained in the previous step and a step size of 0.25 is used as valid to assign to  $\sigma$  the range of values contained in the interval [0.50].

During the intonation of the parameters of the RG, each one of the automatic segmentations of the EDH corresponding to the DB1 described, are compared with the manual segmentations of the EDH generated by a neurosurgeon, considering the  $D_c$ . The optimal values for the parameters of the RG ( $r$  and  $m$ ), are matched to that experiment that generates the highest value for the  $D_c$ .

The  $D_c$  is a metric that allows comparison of segmentations of the same 2D or 3D image, obtained by different methodologies. In the medical context, usually, the  $D_c$  is considered to establish how similar in spatial terms are manual segmentation (RD) and automatic segmentation (RP) in generating the

morphology of any anatomical structure. Additionally, the  $D_c$  is at a maximum when a perfect overlap between RD and RP is reached but it is minimal when RD and RP do not overlap at all. In addition, the expected values for the  $D_c$  are real numbers between 0 and 1. The mathematical model that defines the  $D_c$  is given by Equation 3.

$$D_c = \frac{2|RD \cap RP|}{|RD| + |RP|} \quad (3)$$

In addition, table 1 presents the information related to the parameters obtained after applying the tuning process.

**Table 1. Optimal parameters for the computational algorithms that make up the NLCT.**

MEF (Size)	MF (Size)	RG ( $r,m$ )	MDF (Size)
(3,3,3)	(5,5,5)	(10,6)*	(5,5,5)

\*Values corresponding to the maximum  $D_c=0.9023$  value.

**Obtaining the volumes related to manual segmentations:**

The volume of the hematomas, present in the original images, can be estimated manually by applying the following protocol, applicable only to epidural or intraparenchymal hematomas:

It is assumed that each hematoma, to be characterized, has an ellipsoidal shape. The volume of the hematoma is estimated, considering the axial layers, dividing by 2 the multiplication of the lengths A, B and C; where A and B are the lengths of the major and minor axis of the hematoma, respectively. Such lengths are measured in the image with the "pool" of blood, linked to the hematoma, of greater area. The length C is obtained by multiplying the number of layers, in which the hematoma is present, by the thickness (E) of each layer.

**Obtaining the volumes related to the automatic segmentations:**

The proposed technique generates the automatic segmentations of the EDH present in each of the 7 databases described. From such segmentations, the volume of each hematoma to be characterized, is calculated by multiplying the voxel dimensions by the number of voxels that make up the automatically segmented EDH.

**Clinical utility of the volumes occupied by the hematomas:**

The main clinical utility of the characterization of the hematomas by obtaining the volume lies in the decision-making on the behavior to be followed to address the presence of the hematomas.<sup>24,25</sup>

**Results**

**Quantitative results:** Regarding the trained LSSVM, the values of 2.50 and 0.25, respectively, were obtained as optimal parameters for  $\gamma$  and  $\sigma^2$ . The maximum value of the  $D_c$  obtained for the segmentation of the EDH is comparable with that reported in references<sup>6,8</sup>, as shown in table 2.

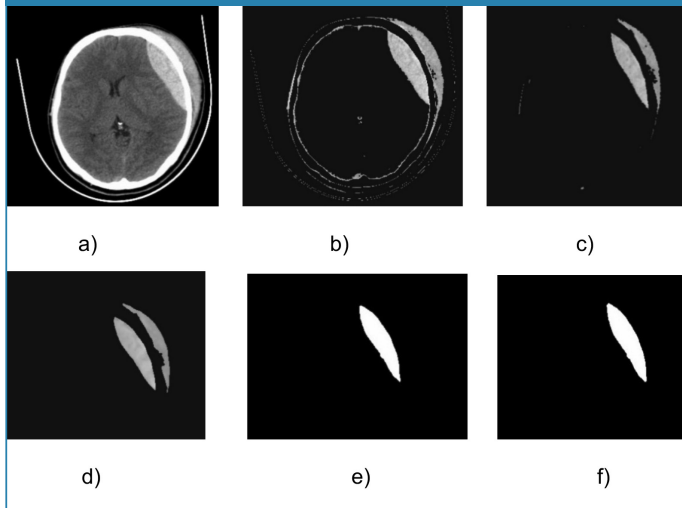
**Table 2. Comparison of the average Dc generated both by the NLCT and other techniques, reported in the literature, for the 3D EDHs segmentation.**

Authors	Technique	Modality	Dc Average
Liao <i>et al.</i> (2010) <sup>6</sup>	(MaxF + PF + MRGP + MRLS)	MSCT	0.9140
Kamnitsas <i>et al.</i> (2017) <sup>8</sup>	Convolutional neural networks	MSCT	0.9037
Vera <i>et al.</i> *	NLCT	MSCT	0.9003

\*This paper's proposed technique.

**Qualitative results:** Figure 3, shows a 2-D view of both the original image and the processed versions after applying the NLCT technique.

**Figure 3. Axial view of images belonging to DB1: a) Original, b) Thresholdized, c) Eroded, d) Median, e) Segmented, f) Postprocessed with the binary morphological dilation filter.**



Additionally, table 3 shows the values for the volume calculated considering the automatic segmentations of the EDHs.

**Table 3. Values obtained for the volume occupied by each of the segmented hematomas.**

Database	Volume (cm <sup>3</sup> )
DB1	9.546
DB2	56.220
DB3	56.893
DB4	30.689
DB5	47.022
DB6	65.041
DB7	23.485

It is important to note that one of the main clinical utilities of these numeric values, for the volumes, is that they crucially determine the conduct to be followed regarding the patient. On the other hand, if only volume is considered, hematomas that exceed the threshold of 30 cm<sup>3</sup> are susceptible to surgery. Following this line, the patients represented by the databases from 2 to 6, according to the calculated volume should be taken to the operating room.

## Conclusions

We have presented a non-linear computational technique whose intonation allows a precise segmentation of cerebral epidural hematomas, present in computed tomography images, since the Dc obtained is comparable to that reported in the literature.

The use of intelligent operators, represented by the least squares support vector machines, allowed for the automatic identification of the coordinates corresponding to the seed voxels that play a crucial role in the adequate initialization of the unsupervised grouping algorithm based on growth of regions.

The segmentations generated, automatically, by the proposed computational technique allow the calculation of the volume of each hematoma considered. This volume is vital when deciding whether a patient is surgically treated or not to address the hematoma.

## Acknowledgements

The authors are grateful for the financial support given by the Universidad Simón Bolívar-Colombia through the 2016-16 code project.

## References

1. Stippler M. Craniocerebral trauma. In: Daroff RB, Jankovic J, Mazziotta JC, Pomeroy SL, eds. *Bradley's Neurology in Clinical Practice*. 7th ed. Philadelphia, PA: Elsevier; 2016: chap 62.
2. Mezzadri J., Goland J., y Sokolovsky M. *Introducción a la Neurocirugía*. Capítulo: Patología vascular II. Ediciones Journal. Segunda edición. 2011.
3. Vera M. Segmentación de estructuras cardiacas en imágenes de tomografía computarizada multi-corte. Ph.D. dissertation, Universidad de los Andes, Mérida-Venezuela, 2014.
4. Maiera A, Wigstrm L, Hofmann H, Hornegger J, Zhu L, Strobel N, Fahrig R. Three-dimensional anisotropic adaptive filtering of projection data for noise reduction in cone beam CT. *Medical Physics*. 2011;38(11):5896–909.
5. Kroft L, De Roos A, Geleijns J. Artifacts in ECG-synchronized MDCT coronary angiography. *American Journal of Roentgenology*. 2007;189(3):581–91.
6. Liao C., Xiao F., Wong J., Chiang I. Computer-aided diagnosis of intracranial hematoma with brain deformation on computed tomography. *Computerized Medical Imaging and Graphics* 34 (2010) 563–571.
7. Dice, L. Measures of the amount of ecologic association between species. *Ecology*, vol. 26, n. 3, pp. 297-302. 1945.
8. Kamnitsas K., Lediga C., Newcombe V., Simpson J., Kaneb A., Menon D., Rueckert D., Glocker B. Efficient Multi-Scale 3D CNN with fully connected CRF for Accurate Brain Lesion Segmentation. *Medical Image Analysis*, Vol 23, pp.1603-1659, 2017.
9. Sezgin M., Sankur B. Survey over image thresholding techniques and quantitative performance evaluation. *Journal of Electronic Imaging*, vol. 13, pp. 146–165, 2004.
10. Pham D., Xu C., Prince J. Current methods in medical image segmentation, *Annual Review of Biomedical Engineering*. vol. 2, pp. 315–337, 2000.

11. Serra J. Image Analysis Using Mathematical Morphology. London, England: Academic Press, 1982.
12. W. Pratt, Digital Image Processing. USA: John Wiley & Sons Inc, 2007.
13. Mukhopadhyay S., Chanda B. A multiscale morphological approach to local contrast enhancement. Signal Processing, vol. 80, no. 4, pp. 685–696, 2000.
14. Yu Z., Wei G., Zhen C., Jing T., Ling L. Medical images edge detection based on mathematical morphology. En Proceedings of the IEEE Engineering in Medicine and Biology 27th Annual Conference, Shanghai–China, September 2005, pp. 6492–6495.
15. Chen T., Wu Q., Rahmani R., Hughes J. A pseudo top-hat mathematical morphological approach to edge detection in dark regions. Pattern Recognition. 2002; 35(1):199–210.
16. Passarielo G., Mora F. Imágenes Médicas, Adquisición, Análisis, Procesamiento e Interpretación. Venezuela: Equinoccio Universidad Simón Bolívar. 1995.
17. Fischer M., Paredes J., Arce G. Weighted median image sharpeners for the world wide web. IEEE Transactions on Image Processing. 2002;11(7):717-27.
18. V. Vapnik, Statistical Learning Theory. New York: John Wiley & Sons, 1998.
19. E. Osuna, R. Freund, y F. Girosi, "Training support vector machines: an application to face detection." en Conference on Computer Vision and Pattern Recognition (CVPR '97), San Juan, Puerto Rico, 1997, pp. 130–136.
20. A. Smola, "Learning with kernels," Tesis de Doctorado, Technische Universitt Berlin, Germany, 1998.
21. B. Scholkopf y A. Smola, Learning with Kernels: Support Vector Machines, Regularization, Optimization, and Beyond. Cambridge, MA, USA: The MIT Press, 2002.
22. J. Suykens, T. V. Gestel, y J. D. Brabanter, Least Squares Support Vector Machines. UK: World Scientific Publishing Co., 2002.
23. M. Oren, C. Papageorgiou, P. Sinha, E. Osuna, y T. Poggio, "Pedestrian detection using wavelet templates," en CVPR '97: Conference on Computer Vision and Pattern Recognition (CVPR '97). Washington, DC, USA: IEEE Computer Society, 1997, pp. 193–200.
24. Hu T., Yan L., Yan Peng., Wang X., Yue G. Assessment of the ABC/2 Method of Epidural Hematoma Volume Measurement as Compared to Computer-Assisted Planimetric Analysis. Biological Research for Nursing. 2016, 18(1) 5-11.
25. Freeman, W., Barrett, K., Bestic, J., Meschia, J., Broderick, D., Brott, T. Computer-assisted volumetric analysis compared with ABC/2 method for assessing warfarinrelated intracranial hemorrhage volumes. 2008, Neurocritical Care, 9, 307–312.

Manuel Velasco (Venezuela) **Editor en Jefe** - Felipe Alberto Espino Comercialización y Producción  
Reg Registrada en los siguientes índices y bases de datos:

**SCOPUS**, EMBASE, Compendex, GEOBASE, EMBiology, Elsevier BIOBASE, FLUIDEX, World Textiles,

**OPEN JOURNAL SYSTEMS (OJS)**, REDALYC (Red de Revistas Científicas de América Latina, el Caribe, España y Portugal),

**Google Scholar**

LATINDEX (Sistema Regional de Información en Línea para Revistas Científicas de América Latina, el Caribe, España y Portugal)

LIVECS (Literatura Venezolana para la Ciencias de la Salud), LILACS (Literatura Latinoamericana y del Caribe en Ciencias de la Salud)

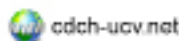
PERIÓDICA (Índices de Revistas Latinoamericanas en Ciencias), REVENCYT (Índice y Biblioteca Electrónica de Revistas Venezolanas de Ciencias y Tecnología)

SABER UCV, DRJI (Directory of Research Journal Indexing)

CLaCaLIA (Conocimiento Latinoamericano y Caribeño de Libre Acceso), EBSCO Publishing, PROQUEST



Esta Revista se publica bajo el auspicio del  
Consejo de Desarrollo Científico y Humanístico  
Universidad Central de Venezuela.



[www.revistahipertension.com.ve](http://www.revistahipertension.com.ve)

[www.revistadiabetes.com.ve](http://www.revistadiabetes.com.ve)

[www.revistasindrome.com.ve](http://www.revistasindrome.com.ve)

[www.revistaavft.com.ve](http://www.revistaavft.com.ve)